

Functional analysis of barley cysteine proteases and their role in nitrogen remobilization from senescing leaves

Fluhr, R. Weizmann Institute of Science

Fischer, A. Montana State University

Project award year: 2016

Three year research project

Abstract

Our work addresses the importance of plastidial protein degradation for agronomically important traits including grain protein concentration and nitrogen use efficiency as contributed by flag leaf senescence. The genetic lines and growth were provided by the US lab, while both lab conducted experiments and jointly analyzed the data. The major findings obtained by the collaborating laboratories over the last three years are the following: 1. Elucidation of transcription factors and secondary metabolites that characterize senescence; 2. Better understanding of the origin and fate of complex and simple carbohydrates during senescence. 3. Establishing the importance of lipid remodeling during senescence in both plastidial and extraplastidial energy metabolism; 4. Analyses of the major cysteine proteases by activity-based profiling of proteases and incorporating that into establishing a general picture of amino acid metabolism and nitrogen transport in senescing flag leaves; 5. Analyses of special cysteine proteases inhibitors, the serpins that turn out to be major proteins in the barley seed that play a non-canonical function in stabilizing beta amylases.

Summary Sheet

Publication Summary

PubType	IS only	Joint	US only
Reviewed	2	0	0

Training Summary

Trainee Type	Last Name	First Name	Institution	Country
Ph.D. Student	Cohen	Maja	WIS	Israel
M.Sc. Student	Hertweck	Kendra	Montana Stae Univ	USA

Contribution of Collaboration

The genetic lines and growth were provided by the US lab, while the Israeli and American labs conducted experiments with the material and jointly analyzed the data. The data and the insights drawn are being prepared for publication. A preliminary draft version with data can be viewed in the Appendix.

Achievements

Transcription factors and secondary metabolites and metabolism: Senescence is a highly regulated process that combines effective molecular breakdown, nutrient remobilization and recycling. It was suggested that more efficient nitrogen remobilization takes place in barley line 10_11 (early senescence; high GPC) while a prolonged carbohydrate accumulation occurs in Karl (delayed senescence; low GPC). Our observations now provide the molecular underpinnings that substantiate this hypothesis. Hence, a coherent model can now be presented for the remobilization of flag leaf constituents in senescing barley. Using RNAseq, we followed senescence initiation factors like transcription factors, hormone pathways and ROS signaling pathways that initiate chloroplast breakdown. The NAC family of transcription factors was shown here to be highly over-represented in senescing barley flag leaves and is involved in developmental senescence and response to biotic and abiotic stresses. Significant induction of the wound-related JA pathway was detected but not the JA hormone itself. Therefore, transcripts identified as part of the initial steps in the JA pathways and that were observed to be up-regulated are likely meant to catalyze general β -oxidation of triacylglycerols (TAGs).

Lipid remodeling during senescence: Using lipid profiling we demonstrated that lipids that accumulate as TAGs are converted to fatty acids and processed by β -oxidation that results in the production of acetyl-CoA and reducing power. Plant vegetative tissues do not normally accumulate significant levels of TAGs; yet, they possess capacity for their synthesis, storage, and metabolism. The de-esterification of thylakoid lipids and the presence of TAGs in stroma plastoglobuli together with accumulation of TAGs during stress and senescence has been shown in Arabidopsis but not in barley. Indeed, genes that encode for enzymes responsible for the acylation of DAGs to TAGs (DGATs) are crucial for the conversion of membrane lipids to TAGs and their activity was shown to be elevated together with enzymes responsible for this process, e.g. TAG, DAG and MAG lipases. Our transcriptomic data showed that these families of enzymes are highly expressed in senescing barley flag leaves. Taken together, TAGs accumulate as a transient pool during the conversion of chloroplast membranes. In this way, lipids stored in TAGs provide energy on demand as a chemically inert buffer between the rapid dismantling of thylakoid membranes and the regulated rate of their use as substrate by β -oxidation in the peroxisome.

Amino acid metabolism during senescence: Degradation pathways of most amino acids were shown to be positively regulated by senescence. Glutamate can be further converted to glutamine by glutamine synthetase 1 (GS1). The cytosolic form of this enzyme was shown to

be up-regulated by senescence. In this scenario, fatty acids originating from chloroplast dismantling would provide the carbon skeletons necessary to the production of glutamine exported to the developing kernels. Comparison between the early (10_11) and late (Karl) senescing barley lines suggests a more efficient metabolism in 10_11. Such metabolism supports higher production of glutamine transported to the grains through amino acid transporters. Hence, one can conclude that upstream mechanisms related to leaf senescence contribute to higher GPC rather than intrinsic differences during the seed fill itself, in other words that barley grain protein accumulation is a source-driven system.

Activity-based profiling of proteases: Chemiluminescent detection of DCG-04-labeled cysteine proteases identified proteins in barley leaves, with much higher activities in girdled than in ungirdled (control) leaves. Mass spectrometric (LC-MS/MS) analysis of three gel fractions (representing the three major as well as adjacent weaker bands) has identified peptides derived from HvPap-6, -7, -8, -12, -14 and -15, indicating that these proteases are active in senescing (girdled) barley leaves, where HvPap-6 is the most active protease. The list of HvPap proteins identified through activity-based profiling of girdled leaves overlaps with the list of HvPap transcripts identified as upregulated through RNA-seq in naturally senescing leaves. Importantly, while 50 barley family C1A cysteine proteases have been identified in the latest barley genome assembly, the number of genes/proteins responsible for protease activity in senescing barley leaves is much smaller.

Special cysteine protease inhibitors: Serpin protease inhibitors and β -amylase starch hydrolases are very abundant seed proteins in the endosperm of grass caryopses. The function of serpins in seeds has yet to be unveiled. In developing endosperm, serpin Z4 and β -amylase showed similar *in vivo* spatio-temporal accumulation properties and co-localize in the cytosol of transformed tobacco leaves. A molecular interaction between recombinant proteins of serpin Z4 and β -amylase was revealed by surface plasmon resonance and microscale thermophoresis. The presence of serpin Z4 stabilized β -amylase activity during heat treatment without affecting its critical denaturing temperature. Oxidative stress, simulated by the addition of CuCl_2 , leads to the formation of high molecular weight polymers of β -amylase similar to those detected *in vivo*. The polymers were cross-linked through disulfide bonds, the formation of which was repressed when serpin Z4 was present. The results suggest an unprecedented function for a plant seed serpin as a β -amylase specific chaperone-like partner that could optimize β -amylase activity upon germination. This is the first report to describe a non-inhibitory function for a serpin in plants.

Publications for Project IS-4915-16 R

Status	Type	Authors	Title	Journal	Vol:pg Year	Count
Published	Reviewed	<i>Cohen M, Fluhr R</i>	Noncanonical interactions between serpin and α -amylase in barley grain improve α -amylase activity in vitro	<i>Plant Direct</i>	2 : 1-12 2018	IS only
Published	Reviewed	<i>Cohen M, Davydov O and Fluhr R</i>	Plant serpin protease inhibitors: specificity and duality of function.	<i>J. Exp Bot</i>	70 : 2077-2085 2019	IS only

Final Scientific Report: Achievements

Functional analysis of barley cysteine proteases and their role in nitrogen remobilization from senescing leaves

Robert Fluhr, Weizmann Institute of Science, Rehovot, Israel

Andreas Fischer, Montana State University, Bozeman, MT, United States

Sections I (research problem and general background) and II (hypotheses, their rationale and research objectives) of the project approved for funding in 2016 provide an overview of barley leaf senescence. These sections specifically address the importance of plastidial protein degradation for agronomically important traits including grain protein concentration and nitrogen use efficiency. The following paragraphs provide a detailed description of the most important findings obtained by the collaborating laboratories over the last three years.

1. Transcription factors and secondary metabolites that characterize senescence

Senescence is triggered by multiple factors, among them phytohormones, transcription factors and reactive oxygen species (ROS)^{1,2}. These factors were used as focal points to analyze the transcriptomic data. NAC, WRKY, MYB, bZIP and bHLH transcription factors showed significant change as a group at 14 and 21 days past anthesis (dpa) in both cv. ‘Karl’ and line ‘10_11’ (Figure 1). The NAC TF family was largely upregulated during senescence with 16 genes upregulated and 4 downregulated in ‘10_11’ whereas 18 were upregulated and 4 downregulated in Karl at 21 dpa. The upregulated transcripts represent a ~twofold enrichment. Our data refine the findings of a survey of NAC transcription factor expression carried out by qPCR during senescence in barley and other plant species^{3,4}. Differential regulation was also found in several other groups of transcription factors, with notable upregulation of several heat stress and ethylene-responsive transcription factors (Figure 1).

Pathways related to the biosynthesis of secondary metabolites like hormones, flavonoids and DIBOA were notably changed (Figure 2). Up-regulation of the jasmonic acid (JA) pathway has been associated with senescence in *Arabidopsis*⁵. As shown here, genes involved in much of the JA biosynthetic pathway in ‘10_11’ were highly induced at 21 dpa, with an 8.4-fold enrichment (p-value = $1.3 \cdot 10^{-11}$), whereas ‘Karl’ showed a 3.7-fold enrichment (p-value = $5.2 \cdot 10^{-3}$). Cytokinins are growth promoting hormones and their level is tightly controlled through

inactivation by O-glucosylation that serves as an antagonist function promoting senescence. Indeed, transcripts associated with cytokinin O-glucosylation were significantly upregulated in '10_11' and 'Karl' (p-value $<4.0 \times 10^{-2}$). Upregulation of the ethylene related pathway has been described as a senescence-promoting factor⁶. However, based on the transcriptomic data of senescing leaves of Karl and 10_11, genes associated with ethylene pathway were not significantly enriched.

Redox balance is essential for cellular homeostasis; decreases in ROS scavengers have been shown to occur during senescence in plants⁷. A reduction in expression of genes associated with L-ascorbate biosynthesis and the ascorbate-glutathione cycle (6 transcripts) is observed in '10_11'. Such a reduction is consistent with the senescence process⁸. The glutathione-mediated detoxification pathway is responsible for the removal of several toxic components and for oxidative stress management⁹. Line '10_11' showed a 2.8-fold enrichment of the glutathione-mediated detoxification pathway between 7 and 21 dpa, while Karl did not (Figure 2B). The accumulation profile of scavengers like ascorbate and glutathione (reduced and oxidized) was analyzed by mass spectrometry in 'Karl'. The contents of ascorbate and glutathione (reduced and oxidized) decreased upon senescence in 'Karl' at 21 dpa (Figure 2C). These results are in accordance with the decline in transcripts related to ascorbate biosynthesis and the ascorbate-glutathione cycle.

Secondary metabolites like flavonoids are known to have efficient anti-oxidant properties in plants¹⁰ while metabolites like DIBOA take part in pathogen defense in cereals¹¹. Both lines showed an enhanced expression of transcripts linked to biosynthesis of flavonoids and DIBOA (p-value <0.05). Similarly, lipid compounds associated with plant defense mechanisms such as phytosterols exhibited a global increase between 7 and 21 dpa in cv. 'Karl' (Figure 2C).

2. Origin and fate of complex and simple carbohydrates

The photosynthetic apparatus is dismantled during senescence, proteins are degraded and nitrogen remobilized to the seed^{1,2,12}. Figure 3A provides the expression profiles of genes associated with photosynthesis and carbon assimilation between 21 and 7 dpa in 'Karl' and '10_11.' Flag leaves from both 'Karl' and '10_11' display a significant decrease in gene expression related to photosynthesis between 7 and 21 dpa. However, most of the carbohydrates detected by mass spectrometry analysis exhibited an increase between 7 and 21 dpa in cv. 'Karl'

(Figure 3B). Besides photosynthesis, sugar levels may also be influenced by starch degradation. The expression of some genes associated with this enzymatic pathway increased with senescence (Figure 3D). Moreover, β -amylase activity was higher in senescing flag leaves at 21 dpa than at 7 dpa (Figure 3C). Hence, it is likely that starch degradation participates in the observed accumulation of carbohydrates such as glucose during senescence.

3. Lipid remodeling during senescence

Transcripts associated with essential chloroplast pathways were shown to decrease during senescence (Figure 3). It was therefore of interest to examine lipid components as these are abundant in the thylakoid membrane system. A total of 122 different lipid metabolites were detected, with 55 of them displaying significant differences between the analyzed stages of senescence in cv. 'Karl' (p -value <0.05). In Figure 4B, lipids are classified into 3 classes; (1) membrane lipids composed of phospho-/galactolipids (PE, lysoPE, PC and MGDG); (2) diacylglycerols (DAG) that are intermediates in the metabolism of both triacylglycerols and membrane lipids; and (3) the energy-rich triacylglycerols (TAGs) which are the main form of fatty acid storage. Strikingly, when comparing senescing flag leaves from 'Karl' between 7 and 14 dpa, most membrane lipids decreased while most TAGs increased. Between 7 dpa and 21 dpa, the lipid profile is similar, with membrane lipids decreasing and most TAGs increasing (Figure 4B).

To visualize TAGs, 'Karl' flag leaves at 21 dpa were stained with Nile Red and BODIPY under a confocal microscope. Both stains bind to neutral lipids and are commonly used to detect lipid droplets. Numerous droplets that co-stained were readily visualized confirming the accumulation of TAGs at this stage (Figure 4D). Thus during senescence, fatty acid constituents of membranes decreased while TAGs increased. These results are consistent with extensive chloroplast degradation and suggest the conversion of its membrane lipids to storage lipids.

Lipid metabolism was also examined at the gene expression level (Figure 4A). Genes related to TAG biosynthesis (glycerol-3-phosphate acyltransferases [GPAT], phosphatidate phosphatases [PAP], acyl-CoA:diacylglycerol acyltransferases [DGAT] and phospholipases [PLA, PLC] were identified and found to be mainly upregulated between 21 and 7 dpa. In parallel, the TAG degradation pathway involving lipases was found to be highly upregulated (Figure 4C, steps 5-7). Fatty acid products of TAGs enter the peroxisome where they are further metabolized to produce reducing power and acetyl-CoA. Taken together, the transcriptomic and metabolomic

results are consistent with massive chloroplast membrane dismantling and synthesis of TAGs during senescence. Hence, in the absence of photosynthesis-based energy metabolism, membrane lipids are converted to transient storage as TAGs, maintaining reducing power and providing carbon backbones.

4. *Extraplasmidial energy metabolism*

To further analyze changes in energy metabolism, extraplasmidial metabolic pathways were inspected in terms of gene expression and metabolic profiling (Figure 5). During glycolysis, glucose is utilized to reduce NAD, create ATP and supply pyruvate to fuel the TCA cycle. However, genes associated with glycolysis were mostly downregulated when comparing young flag leaves (7 dpa) to older ones (14 and 21 dpa) in both barley lines analyzed (Figure 5A). Moreover, phosphoenolpyruvate (PEP) and pyruvate levels decreased during senescence of ‘Karl’ barley flag leaves (Figure 5B). Genes associated with the TCA cycle exhibited a mixed pattern of expression. Interestingly, the levels of the two TCA cycle metabolic intermediates, aconitate and isocitrate, decreased upon senescence.

In contrast, expression of almost all of the genes related to fatty acid β -oxidation increased by at least 1.8-fold between 7 and 21 dpa in both ‘Karl’ and ‘10_11’ (Figure 5A). It is worthwhile to note that many of the genes associated with peroxisomal activity are also needed for jasmonic acid biosynthesis (Figure 2A). Still, peroxisomal/glyoxysomal activity, where fatty acids are converted to reducing power (NADH, FADH₂) and acetyl-CoA, showed clear up-regulation (Figure 5A). Acetyl-CoA can be used by the glyoxylate cycle to produce *inter alia* citrate and glyoxylate. Two central genes in the glyoxylate cycle are malate synthase and isocitrate lyase, denoted by steps 7 and 8 in Figure 5. The significance of those genes is emphasized by their lack of redundancy. Hence, the strong upregulation of both genes at 21 dpa compared to 7 dpa in both ‘Karl’ and ‘10_11’ highlights the importance of peroxisome/glyoxysome metabolism during the senescence process (Figure 5).

The glyoxylate cycle usually cooperates with gluconeogenesis to produce carbohydrates from fatty acids. Transcriptomic analysis of senescing flag leaves indicated that genes associated with gluconeogenesis are mostly down-regulated (steps 2, 11-13, Figure 5A); therefore, the glyoxylate cycle may provide carbon backbones for other purposes such as the TCA cycle. Carbon is thought to exit the peroxisome as citrate^{13,14} to be converted to isocitrate in the cytosol and sent

back to the peroxisome to complete the glyoxylate cycle. Alternatively, cytosolic isocitrate can be converted to 2-OG by the enzyme isocitrate dehydrogenase (ICDH) in the cytosol. Citrate can also be imported by the mitochondria and further converted to 2-OG as a part of the TCA cycle. Of these possibilities, the expression of several transcripts encoding ICDH exhibited an increase between 7 and 21 dpa (step 9, Figure 5A/B). Interestingly, several mitochondrial solute carriers from the SLC 25 family¹⁵ exhibited an increase in their expression upon senescence. For example, the mitochondrial 2-OG transporter encoded by HORVU5Hr1G078950 showed a 2 fold induction upon senescence and could contribute to the exchange of TCA intermediates like 2-OG and citrate between the cytosol and mitochondria (step 10, Figure 5).

5. *Proteolytic enzymes in senescing flag leaves*

Groups of protease genes were found to be differentially expressed during senescence (Figure 6). Among them a majority of differentially regulated cysteine protease genes are upregulated, while the distribution between up-and downregulated genes is more even for the other protease classes (Figure 6). We also identified upregulated protease inhibitors including three cystatins in line '10_11.' Furthermore, a Clp protease adapter protein (ClpS) was upregulated >20-fold in both 'Karl' and line '10_11' at 21 days; this protein may have a role in regulating plastidial proteolysis.

To examine cysteine proteases at the protein and activity levels, two prominent members of the C1A family, HvPap-6 (RD21 barley ortholog) and HvPap-12 (aleurain), were monitored by immunoblotting and enzymatic assays at 7, 14 and 21 dpa (Figure 7). At 7 dpa, HvPap-6 was mainly found in its immature form (band indicated by a blue arrow). As senescence progressed, the immature enzyme was cleaved to yield the mature form of the protease at 21 dpa. An increase in total HvPap-6 protein between 7 and 21 dpa can be observed as pre-pro (white arrow) and mature (red arrow) enzyme in both barley lines. The two membranes shown in Figure 7A were exposed to the same treatments and same exposure time. It seems that there were more pre-pro and mature HvPap-6 in line '10_11' as compared to cv. 'Karl.' To directly measure the proteolytic activity in the senescing leaves, a specific fluorogenic substrate preferentially cleaved by RD21, KLR:AMC was used¹⁶. Cysteine proteases were significantly more active at 21 dpa compared to earlier time points and significantly more active in line '10_11' as compared to Karl using this substrate (Figure 7B).

Aleurain (HvPap-12) is produced as a zymogen (pro-aleurain) and activated by limited proteolysis to generate a mature enzyme. Moreover, it was reported that HvPap-6/RD21 may be one of the enzymes responsible for its maturation¹⁷. As HvPap-6 was elevated in line '10_11' we probed aleurain maturation patterns. In Figure 7C, specific anti-aleurain peptide antibodies were used. It is apparent that the immature aleurain (white arrow) was cleaved to its mature form (red arrow) between 7 and 14 dpa in both lines. Moreover, by 14 dpa the pre/pro form of aleurain was mostly processed in line '10_11' but not in cv. 'Karl.' No gradual increase in protein content (immature or mature) was observed during senescence while the transcript levels showed a twofold increased between 7 and 21 dpa. Interestingly, enzyme activity levels measured with the fluorogenic substrate RR:AMC were significantly higher at 14 and 21 as compared to 7 dpa for both lines. Furthermore, detected activities were higher in line '10_11' than in 'Karl' at 14 and 21 dpa (Figure 7D). These results are consistent with the immunoblot indicating that aleurain maturation occurred mostly between 7 and 14 dpa. Transcriptomic analysis indicated a 2.3/3.2-fold upregulation of HvPap-6/RD21, and a 1.3/2.0-fold upregulation of HvPap-12/aleurain in leaves of 'Karl' and '10_11' at 21 vs. 7 days, but data presented in Figure 7 demonstrate that post-translational regulation is also important for appreciating the difference between the two lines.

6. Activity-based profiling of cysteine proteases

Cysteine protease biochemistry was also probed using activity-based profiling, a targeted proteomic approach. To develop this method, the leaf girdling technique was applied which allows the production of large quantities of evenly senesced leaf blades from young barley plants (Fig. 8A)¹⁸⁻²¹. Proteases extracted from senescing leaves were labeled using DCG-04, a molecule derived from the commonly used protease inhibitor E-64²² complemented with a linker and a biotin tag allowing protease detection and purification²³. Results from activity-based profiling of cysteine proteases are as follows:

- Chemiluminescent detection of DCG-04-labeled cysteine proteases identifies three bands in barley leaves, with much higher activities in girdled than in ungirdled (control) leaves (Figure 8B). Protease bands are not detected when samples are incubated with excess (with respect to DCG-04) E-64, indicating that these bands represent specific labeling of cysteine proteases by the utilized probe (Fig. 8B).

- Affinity purification (using streptavidin-agarose beads) of biotin-tagged cysteine proteases from 8-day girdled leaves, followed by SDS-PAGE separation identifies three major and at least two minor bands, most likely representing pre-proteins and mature forms of several cysteine proteases (Fig. 8C).
- Mass spectrometric (LC-MS/MS) analysis of three gel fractions (representing the three major as well as adjacent weaker bands) has identified peptides derived from HvPap-6, -7, -8, -12, -14 and -15, indicating that these proteases are active in senescing (girdled) barley leaves. Numbers of different peptides detected, as well as spectral counts per peptide, suggest that HvPap-6 is the most active protease in our samples, followed by HvPap-12 and -14 (data for HvPap-6 are shown in Fig. 9). It may be noted that direct MS analysis of affinity-purified samples (omitting the gel separation) identified fewer proteases, but HvPap-6 was again the most dominant enzyme.

The list of HvPap proteins identified through activity-based profiling of girdled leaves overlaps with the list of *HvPap* transcripts identified as upregulated through RNA-seq in naturally senescing leaves (Figure 6). Therefore, while 50 barley family C1A cysteine proteases have been identified in the latest barley genome assembly²⁴, the number of genes/proteins responsible for protease activity in senescing barley leaves is much smaller, making the system more amenable to detailed study and manipulation in future projects.

7. *Amino acid metabolism and nitrogen transport in senescing flag leaves*

One might expect that the increased proteolytic activity that characterizes senescing tissue would lead to an increase in amino acid pools; however, the opposite has been observed²⁵. In our experiments, the levels of all amino acids that were detected were lower at 21 dpa in cv. 'Karl' (Figure 10A). Numerous genes coding for enzymes involved in transamination and amino acid degradation were increased during senescence, while a smaller number were downregulated (Figure 10B). Upregulation occurred more prominently in (early-senescing) line '10_11' than in cv. 'Karl', and mostly at 21 days, indicating that these are functions that are important during later senescence stages. Transcriptomic data suggest strong upregulation of multiple genes involved in arg/pro, branched-chain, lys and aromatic amino acid catabolism at 21 days (Figure 10B), using a recent review on plant amino acid catabolism as a guide²⁶ for gene analysis.

Amino acids and possibly peptides resulting from proteolysis and amino acid metabolism need to be transported to the developing seeds via the phloem. Our transcriptomic analysis has identified upregulation of numerous genes coding for membrane transport proteins including seven putative amino acid permeases, three oligopeptide transport proteins, and four transmembrane amino acid transport proteins, while a smaller number of transport genes/proteins were downregulated (Figure 10C). The combination of transcriptomic and metabolomic data therefore indicates active amino acid metabolism and transport functions, with the latter explaining decreasing amino acid levels in senescing barley leaves (Figure 10A). Similarly to our protease results, data shown in Fig. 10 will facilitate future studies aimed at dissecting the metabolism and transport of amino acids resulting from the degradation of (mostly) plastidial proteins during senescence.

A diagram summarizing and interpreting our findings from this study is shown in Figure 11.

8. Literature cited in this report:

- 1 Fischer, A. M. The complex regulation of senescence. *Crit. Rev. Plant Sci.* **31**, 124-147 (2012).
- 2 Distelfeld, A., Avni, R. & Fischer, A. M. Senescence, nutrient remobilization, and yield in wheat and barley. *J. Exp. Bot.* **65**, 3783-3798, doi:10.1093/jxb/ert477 (2014).
- 3 Christiansen, M. W. *et al.* Barley plants over-expressing the NAC transcription factor gene HvNAC005 show stunting and delay in development combined with early senescence. *J. Exp. Bot.* **67**, 5259-5273, doi:10.1093/jxb/erw286 (2016).
- 4 Podzimska-Sroka, D., O'Shea, C., Gregersen, P. L. & Skriver, K. NAC Transcription Factors in Senescence: From Molecular Structure to Function in Crops. *Plants* **4**, 412-448, doi:10.3390/plants4030412 (2015).
- 5 He, Y., Fukushige, H., Hildebrand, D. F. & Gan, S. Evidence Supporting a Role of Jasmonic Acid in Arabidopsis Leaf Senescence. *Plant Physiol.* **128**, 876-884, doi:10.1104/pp.010843 (2002).
- 6 Kim, J., Chang, C. & Tucker, M. L. To grow old: regulatory role of ethylene and jasmonic acid in senescence. *Frontiers in Plant Science* **6**, doi:10.3389/fpls.2015.00020 (2015).
- 7 Rogers, H. & Munné-Bosch, S. Production and Scavenging of Reactive Oxygen Species and Redox Signaling during Leaf and Flower Senescence: Similar But Different. *Plant Physiol.* **171**, 1560-1568, doi:10.1104/pp.16.00163 (2016).
- 8 Zimmermann, P. & Zentgraf, U. The correlation between oxidative stress and leaf senescence during plant development. *Cellular and Molecular Biology Letters* **10**, 515 (2005).
- 9 Chronopoulou, E. *et al.* in *Glutathione in Plant Growth, Development, and Stress Tolerance* (eds Mohammad Anwar Hossain *et al.*) 215-233 (Springer International Publishing, 2017).
- 10 Samanta, A., Das, G. & Das, S. *Roles of flavonoids in Plants*. Vol. 6 (2011).
- 11 Mikić, S. & Ahmad, S. Benzoxazinoids-protective secondary metabolites in cereals: Biochemistry and genetic control. *Ratarstvo i povrtarstvo* **55**, 39-48 (2018).

- 12 Liu, J., Wu, Y. H., Yang, J. J., Liu, Y. D. & Shen, F. F. Protein degradation and nitrogen remobilization during leaf senescence. *Journal of Plant Biology* **51**, 11-19, doi:10.1007/BF03030735 (2008).
- 13 Kaur, N., Cross, L., Theodoulou, F. L., Baker, A. & Hu, J. Plant peroxisomes: protein import, dynamics, and metabolite transport. *Plant Cell Biology*, 1-24 (2016).
- 14 Kunze, M., Pracharoenwattana, I., Smith, S. M. & Hartig, A. A central role for the peroxisomal membrane in glyoxylate cycle function. *Biochim. Biophys. Acta* **1763**, 1441-1452, doi:<https://doi.org/10.1016/j.bbamcr.2006.09.009> (2006).
- 15 Palmieri, F. The mitochondrial transporter family (SLC25): physiological and pathological implications. *Pflügers Archiv* **447**, 689-709, doi:10.1007/s00424-003-1099-7 (2004).
- 16 Cohen, M., Davydov, O. & Fluhr, R. Plant serpin protease inhibitors: specificity and duality of function. *J. Exp. Bot.* **70**, 2077-2085 (2019).
- 17 Halls, C. E., Rogers, S. W. & Rogers, J. C. Purification of a proaleurain maturation protease. *Plant Sci.* **168**, 1267-1279, doi:<https://doi.org/10.1016/j.plantsci.2005.01.004> (2005).
- 18 Feller, U. & Fischer, A. Nitrogen metabolism in senescing leaves. *Crit. Rev. Plant Sci.* **13**, 241-273, doi:10.1080/07352689409701916 (1994).
- 19 Parrott, D., Yang, L., Shama, L. & Fischer, A. M. Senescence is accelerated, and several proteases are induced by carbon "feast" conditions in barley (*Hordeum vulgare* L.) leaves. *Planta* **222**, 989-1000, doi:10.1007/s00425-005-0042-x (2005).
- 20 Parrott, D. L., McInnerney, K., Feller, U. & Fischer, A. M. Steam-girdling of barley (*Hordeum vulgare*) leaves leads to carbohydrate accumulation and accelerated leaf senescence, facilitating transcriptomic analysis of senescence-associated genes. *New Phytol.* **176**, 56-69, doi:10.1111/j.1469-8137.2007.02158.x (2007).
- 21 Parrott, D. L., Martin, J. M. & Fischer, A. M. Analysis of barley (*Hordeum vulgare*) leaf senescence and protease gene expression: a family C1A cysteine protease is specifically induced under conditions characterized by high carbohydrate, but low to moderate nitrogen levels. *New Phytol.* **187**, 313-331, doi:10.1111/j.1469-8137.2010.03278.x (2010).
- 22 Hanada, K. *et al.* Isolation and characterization of E-64, a new thiol protease inhibitor. *Agric. Biol. Chem.* **42**, 523-528, doi:10.1080/00021369.1978.10863014 (1978).
- 23 Greenbaum, D., Medzihradszky, K. F., Burlingame, A. & Bogyo, M. Epoxide electrophiles as activity-dependent cysteine protease profiling and discovery tools. *Chem. Biol.* **7**, 569-581, doi:10.1016/S1074-5521(00)00014-4 (2000).
- 24 Mascher, M. *et al.* A chromosome conformation capture ordered sequence of the barley genome. *Nature* **544**, 427-433, doi:10.1038/nature22043 (2017).
- 25 Avila-Ospina, L., Clément, G. & Masclaux-Daubresse, C. Metabolite profiling for leaf senescence in barley reveals decreases in amino acids and glycolysis intermediates. *Agronomy* **7**, 15 (2017).
- 26 Hildebrandt, T. M., Nunes Nesi, A., Araújo, W. L. & Braun, H.-P. Amino acid catabolism in plants. *Mol. Plant* **8**, 1563-1579, doi:10.1016/j.molp.2015.09.005 (2015).

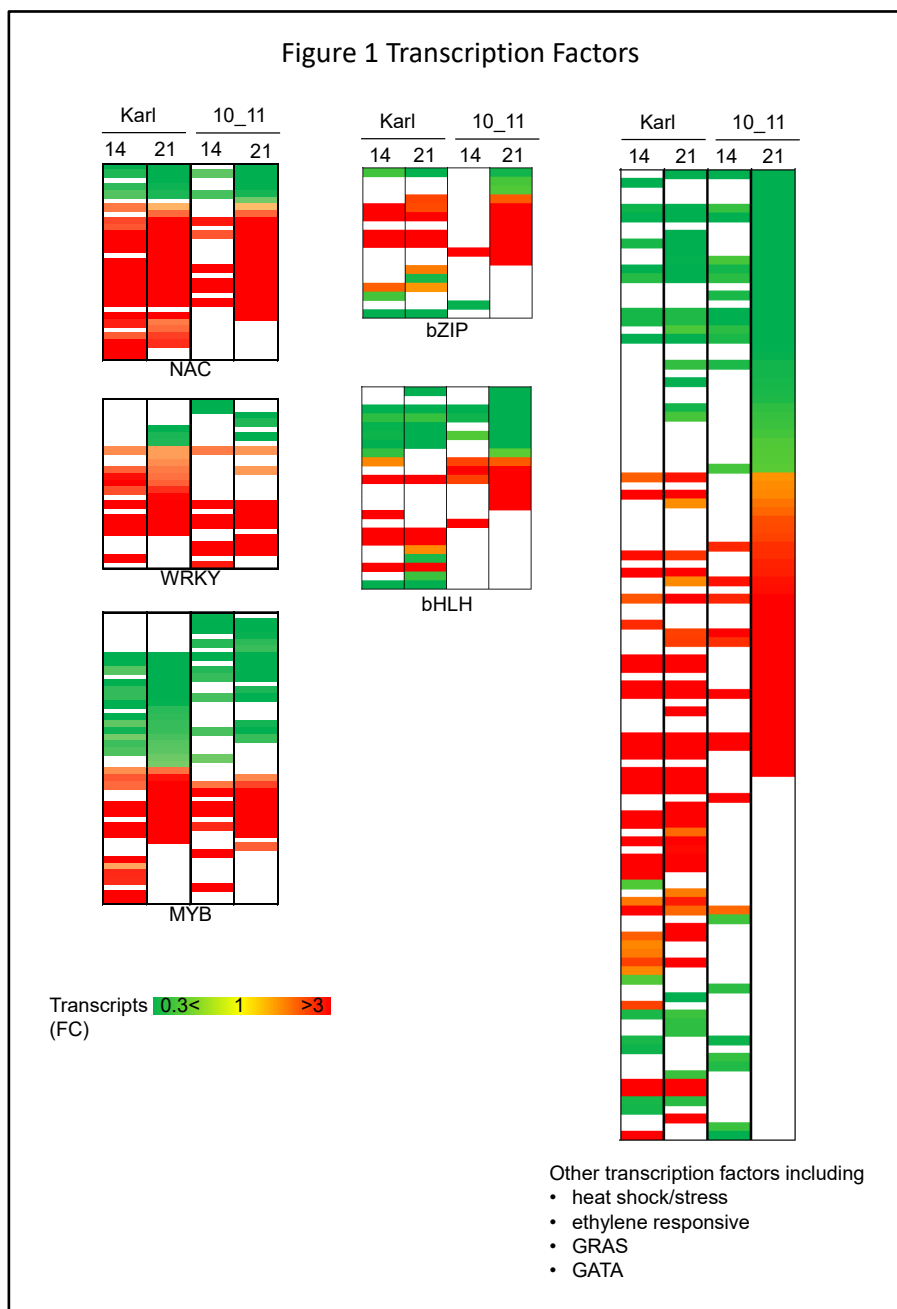


Figure 1. Transcription factors. Marseq analysis was performed on senescing flag leaves from cv. 'Karl' and its near-isogenic line '10-11' at 7, 14 and 21 days past anthesis (dpa). The expression profiles of genes coding for transcription factors are shown; values represent –fold changes (FC) at 14 vs. 7 dpa, and at 21 vs 7 dpa. Values >1 indicate upregulation at the later time point, i.e., with progressing leaf senescence. Only genes/time points with FC >1.8 or FC <0.55 with $p < 0.05$ are shown.

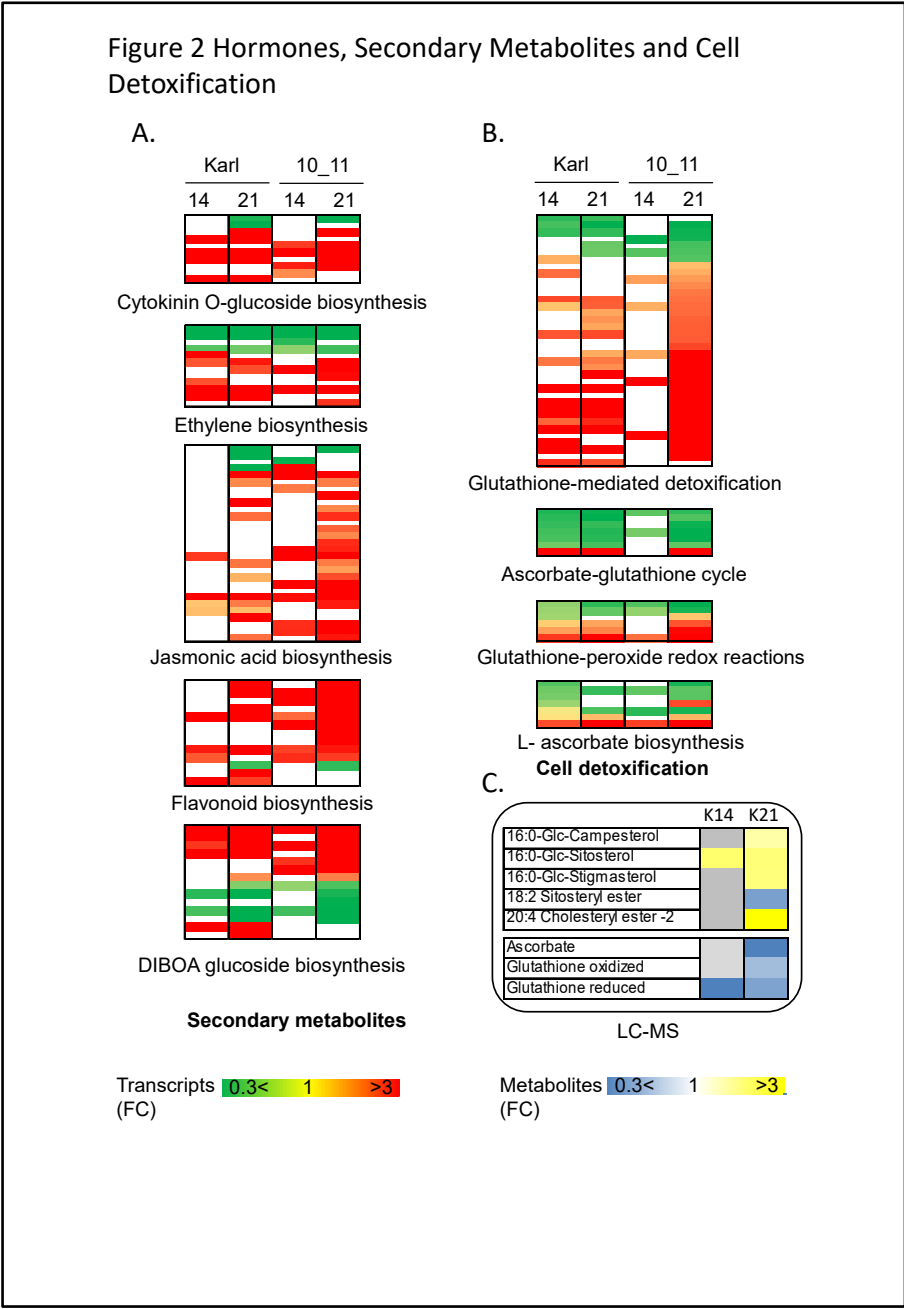


Figure 2. Hormones, secondary metabolites and cell detoxification. Marseq analysis was performed on senescing flag leaves from cv. ‘Karl’ and its near-isogenic line ‘10-11’ at 7, 14 and 21 days past anthesis (dpa). Gene expression values (A, B) represent –fold changes(FC) at 14 vs. 7 dpa, and at 21 vs. 7 dpa. Values >1 indicate upregulation at the later time point, i.e., with progressing leaf senescence. Only genes/time points with FC >1.8 or FC <0.55 with p <0.05 are shown. Phytosterol and redox compound profiling (C) was performed on senescing flag leaves from cv. ‘Karl’ at 7, 14 and 21 dpa; data are shown as for transcripts.

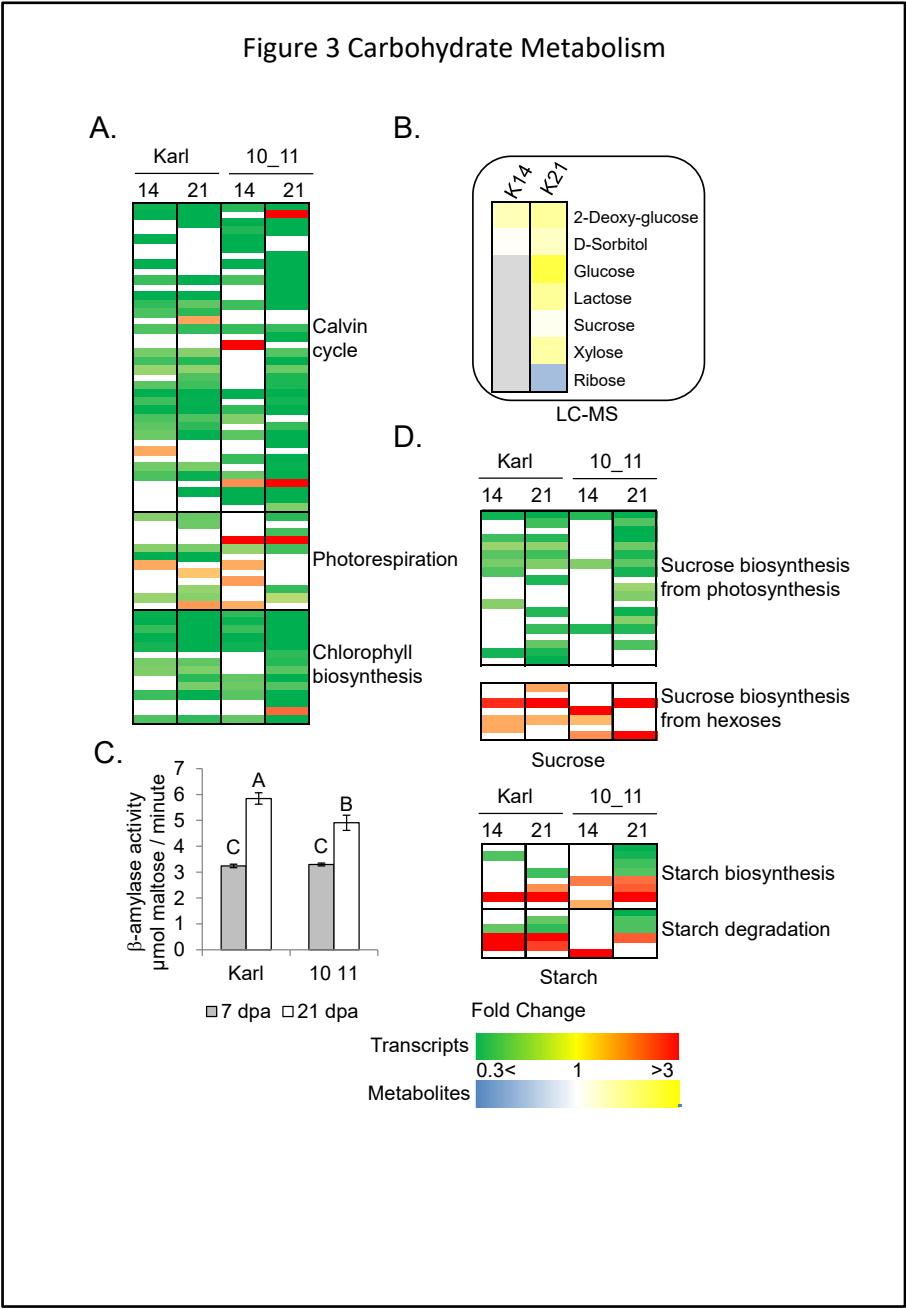


Figure 3. Carbohydrate metabolism. Marseq analysis was performed on senescing flag leaves from cv. ‘Karl’ and its near-isogenic line ‘10-11’ at 7, 14 and 21 days past anthesis (dpa). The expression profiles of genes coding for enzymes involved in photosynthesis (A), sucrose and starch metabolism (D) are shown. Values represent –fold changes (FC) at 14 vs. 7 dpa, and at 21 vs 7 dpa. Values >1 indicate upregulation at the later time point, i.e., with progressing leaf senescence. Only genes/time points with FC >1.8 or FC <0.55 with p <0.05 are shown. Metabolite (carbohydrate) profiling (B) was performed on senescing flag leaves from cv. ‘Karl’ at 7, 14 and 21 dpa; data are shown as for transcripts. Results of β -amylase activity assays are shown in panel C.

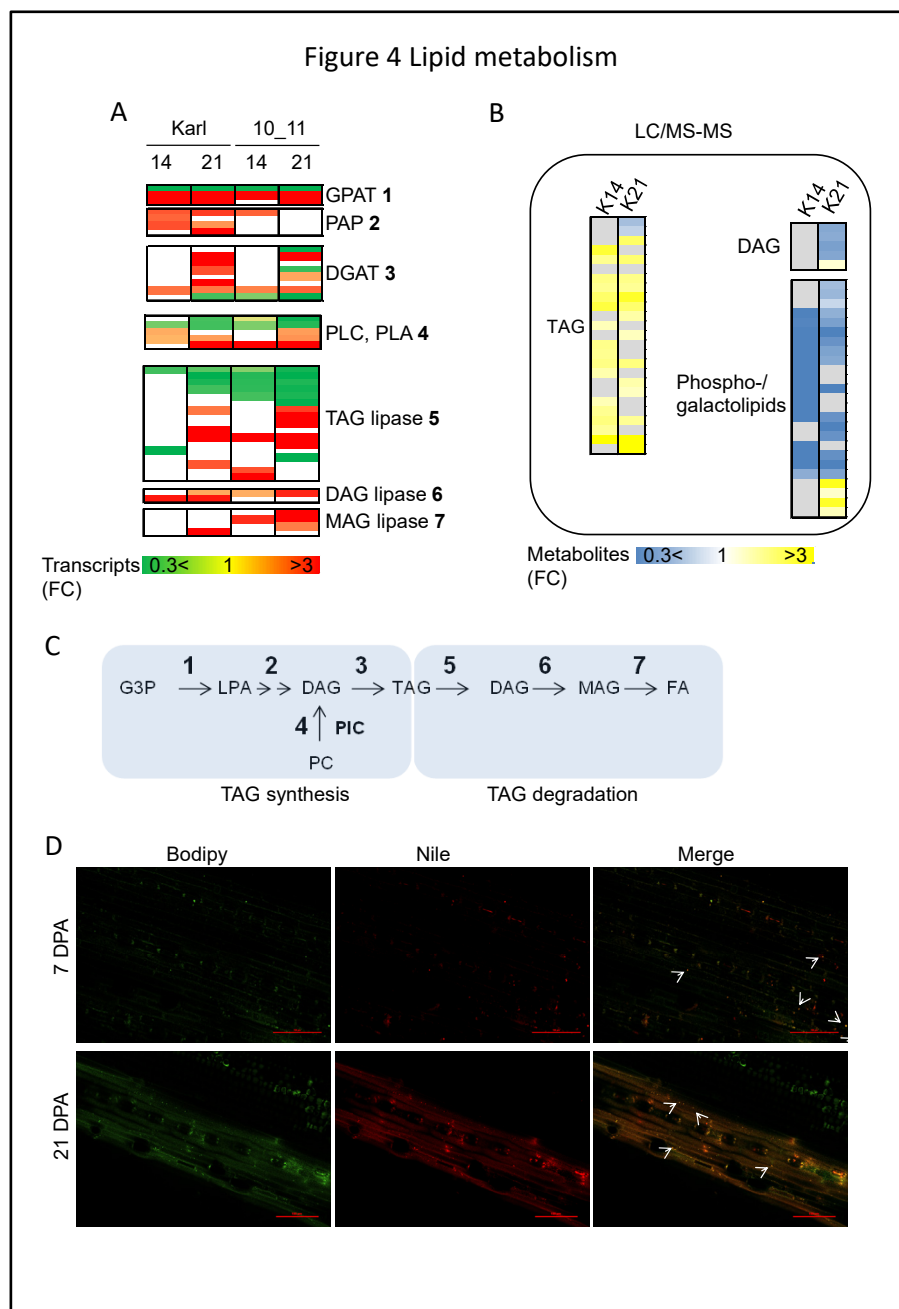


Figure 4. Lipid metabolism. Marseq analysis was performed on senescing flag leaves from cv. ‘Karl’ and its near-isogenic line ‘10-11’ at 7, 14 and 21 days past anthesis (dpa). The expression profiles of genes coding for enzymes involved in triacylglycerol (TAG) synthesis and degradation were inspected (A). Values represent – fold changes (FC) at 14 vs. 7 dpa, and at 21 vs 7 dpa. Values >1 indicate upregulation at the later time point, i.e., with progressing leaf senescence. Only genes/time points with FC >1.8 or FC <0.55 with $p < 0.05$ are shown. Metabolite (lipid) profiling (B) was performed on senescing flag leaves from cv. ‘Karl’ at 7, 14 and 21 dpa; data are presented as for transcripts. Panel D shows Nile Red and BODIPY staining of senescing flag leaves from cv. ‘Karl’ at 7 and 21 dpa. White arrows indicate lipid droplets. At least 15 images from at least 5 flag leaves per age sample were analyzed by confocal microscopy; typical images are shown.

GPAT, glycerol-3-phosphate acyltransferase; PAP, phosphatidic acid phosphatase; PIC, PLA, phospholipases A and C; DAG, diacylglycerol; MAG, monoacylglycerol. Numbers in panel A point to enzymatic steps in panel C.

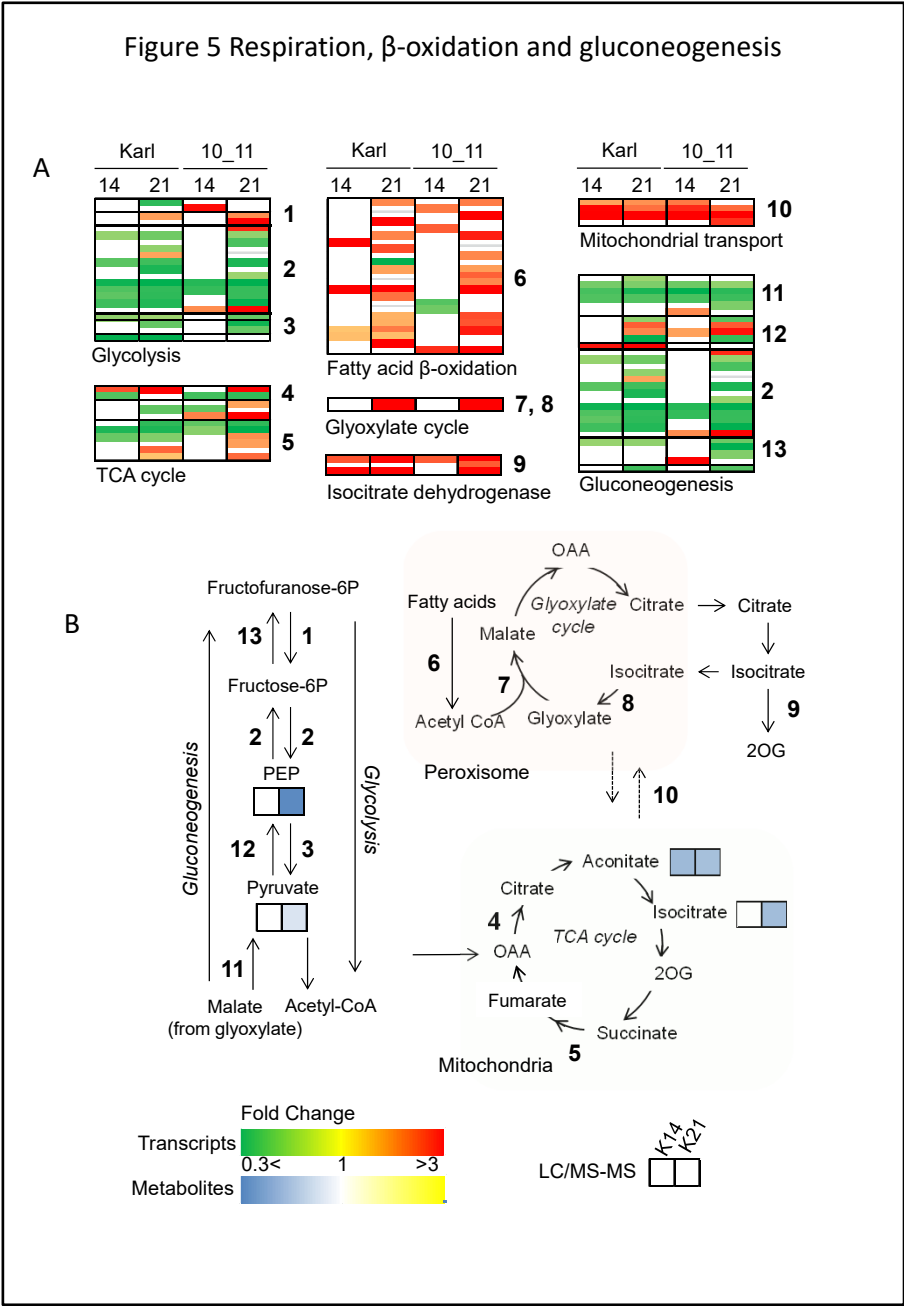


Figure 5. Respiration, β -oxidation and gluconeogenesis. Marseq analysis was performed on senescing flag leaves from cv. ‘Karl’ and its near-isogenic line ‘10-11’ at 7, 14 and 21 days past anthesis (dpa). Values represent –fold changes (FC) in transcript levels at 14 vs. 7 dpa, and at 21 vs 7 dpa. Values >1 indicate upregulation at the later time point, i.e., with progressing leaf senescence. Only genes/time points with FC >1.8 or FC <0.55 with p <0.05 are shown. Numbers in panel B indicate enzymatic steps catalyzed by genes analyzed in (A), with levels of four metabolites identified also shown.

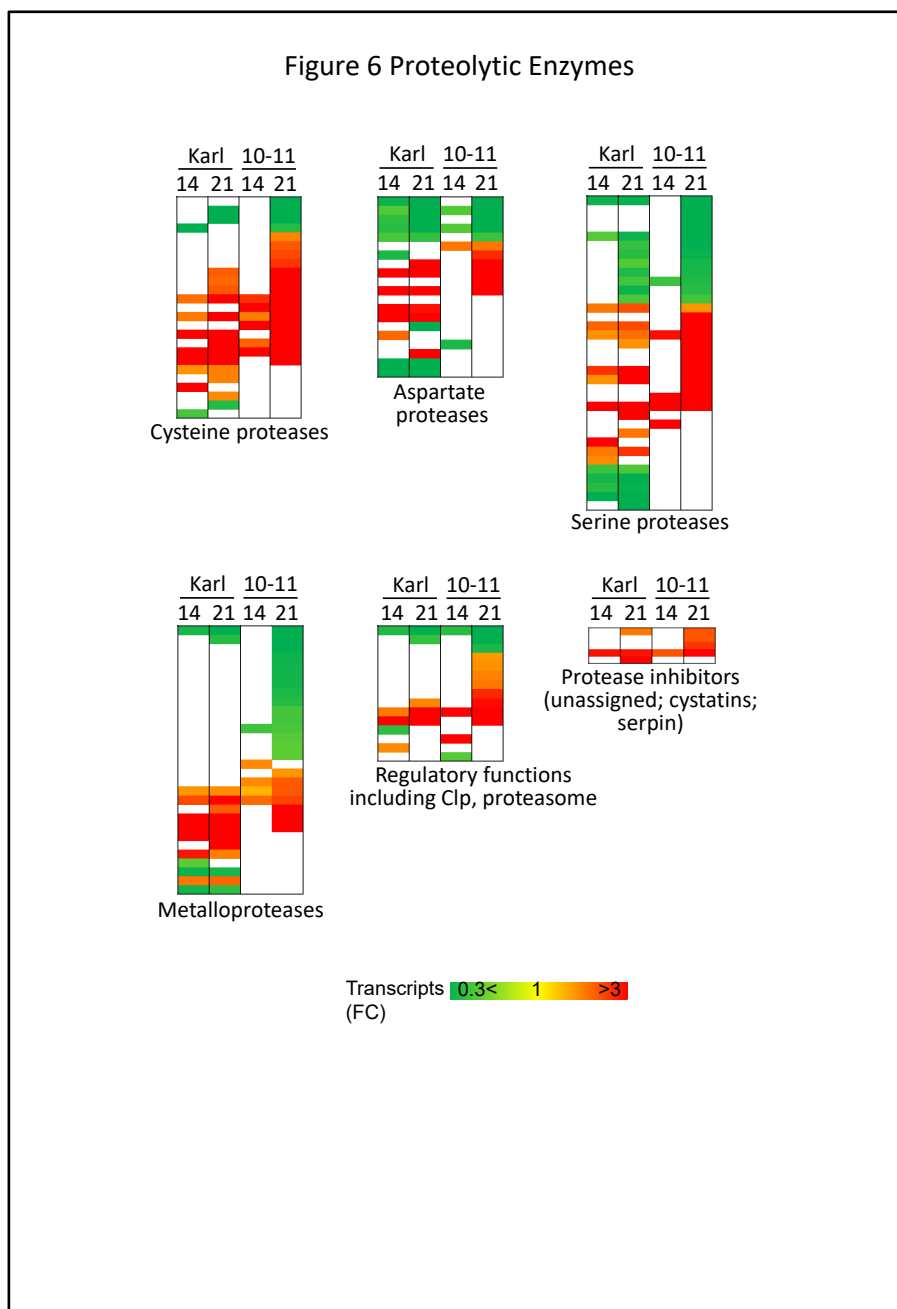


Figure 6. Proteolytic enzymes. Marseq analysis was performed on senescing flag leaves from cv. 'Karl' and its near-isogenic line '10-11' at 7, 14 and 21 days past anthesis (dpa). The expression profiles of genes coding for proteases or for proteins involved in protease regulation were inspected. Values represent –fold changes (FC) at 14 vs. 7 dpa, and at 21 vs 7 dpa. Values >1 indicate upregulation at the later time point, i.e., with progressing leaf senescence. Only genes/time points with FC >1.8 or FC <0.55 with $p < 0.05$ are shown.

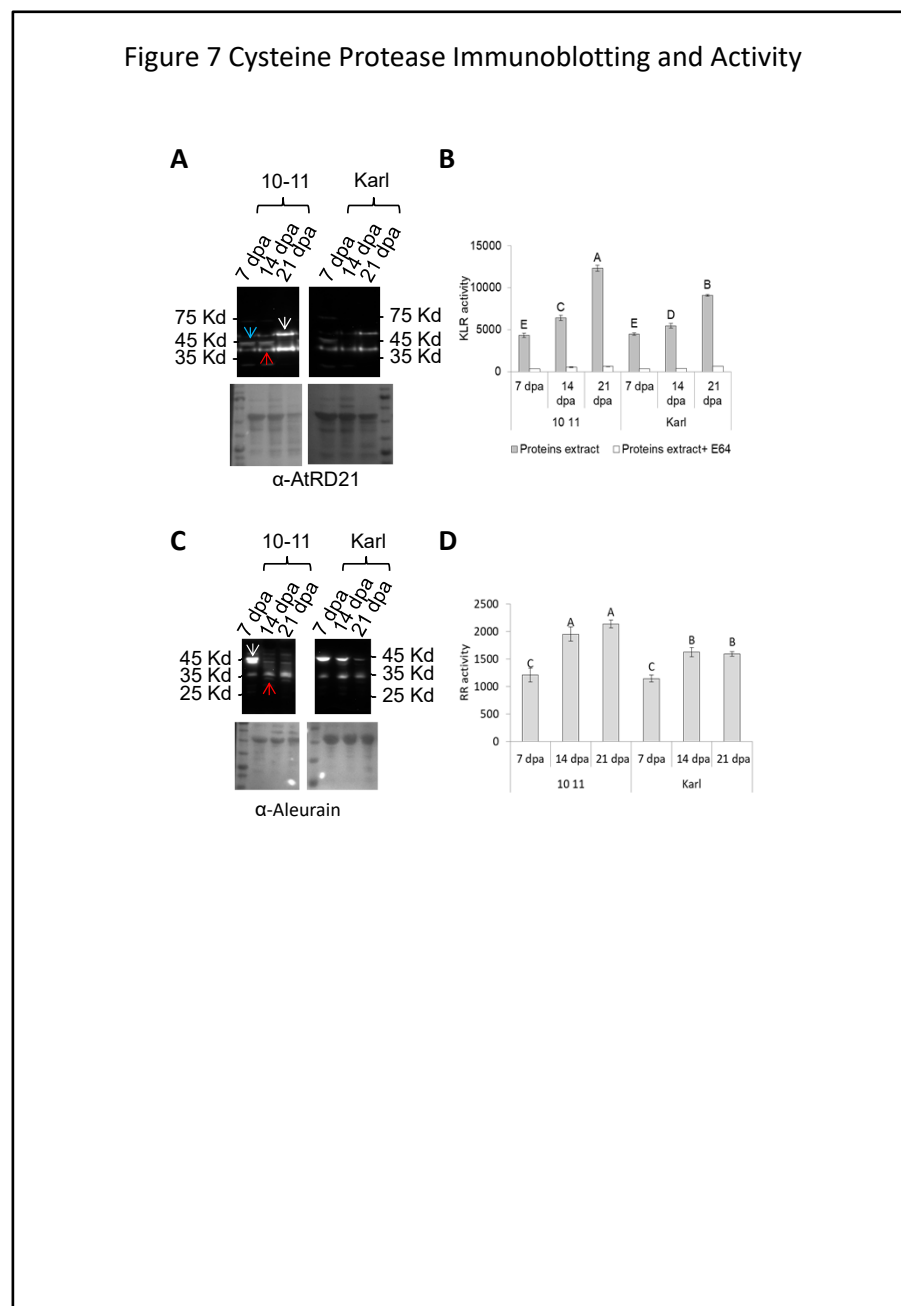


Figure 7. Cysteine protease immunoblotting and activity. Immunoblots were prepared from flag leaves of cv. 'Karl' and its near-isogenic line '10-11,' separating 50 µg of protein per lane (A, C). *Arabidopsis* anti-RD21 antibodies were used for detection in panel A, while antibodies against barley aleurain were used in panel C. Arrows indicate immature (white, blue) and mature (red) isoforms in panel A, while white and blue arrows designate immature and mature forms, respectively, in panel C. Proteolytic activities against fluorogenic substrates were analyzed for data shown in panels B (KLR:AMC) and D (RR:AMC). The cysteine protease inhibitor E-64 was used at 100 µM in B to confirm that measured activity was caused by cysteine proteases. Experiments are based on three biological replicates.

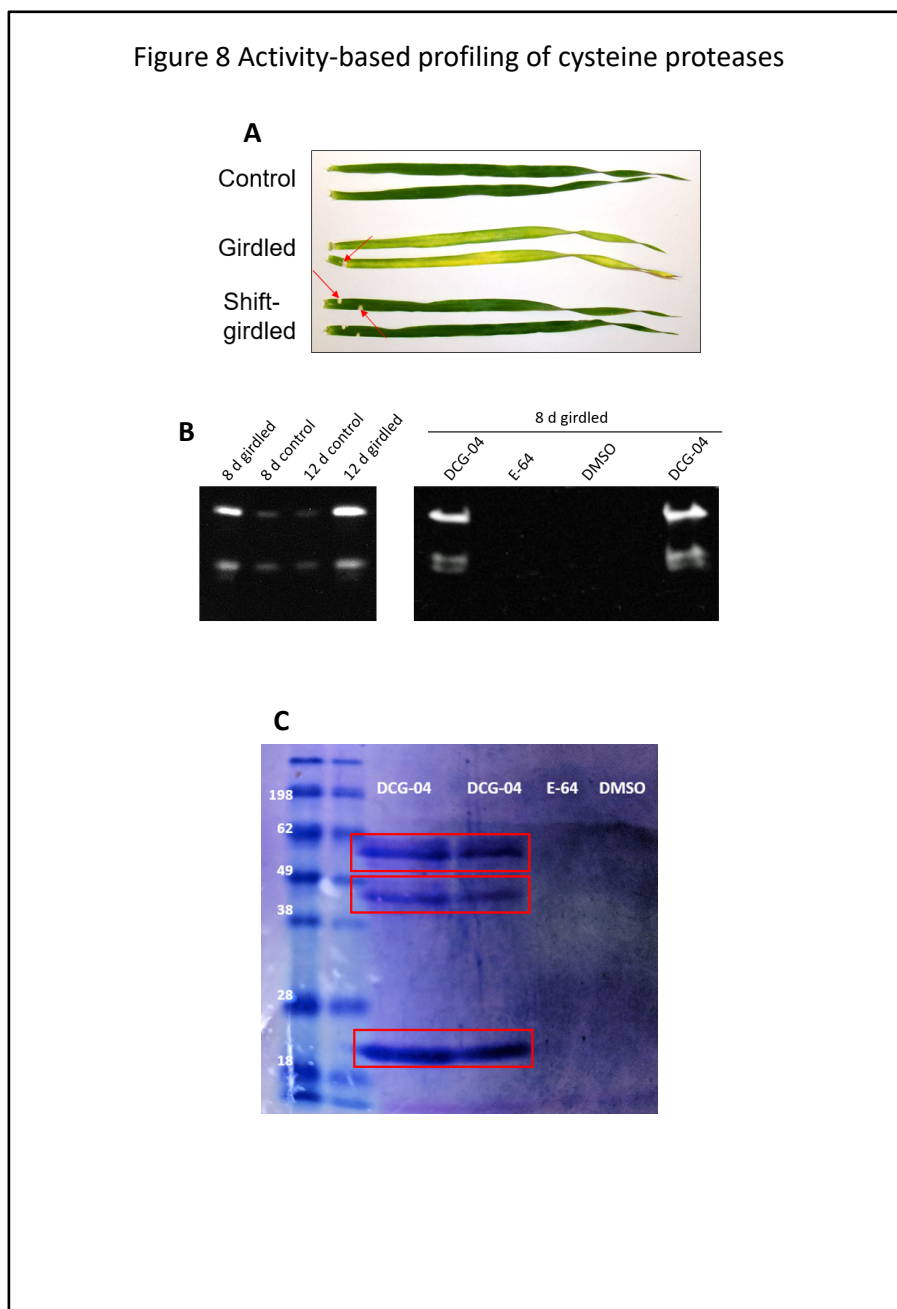


Figure 8. Activity-based profiling of cysteine proteases. A. Interruption of the phloem at the basis of the leaf blade through steam-girdling leads to accelerated senescence. Note that the girdling zone needs to cross the entire width of the leaf; shift-girdled leaves (bottom) behave like ungirdled controls (top). Leaves are shown at 12 days after treatment; they were removed from intact plants immediately prior to documentation. Red arrows point to girdling zones, highlighting the necrotic tissue. B. Active cysteine proteases were characterized using the activity probe DCG-04, followed by detection using streptavidin-horseradish peroxidase. No bands were detected in presence of E-64 and in absence of DCG-04 (DMSO), confirming that labeling is specific for cysteine protease activity. C. DCG-04 labeled cysteine proteases were affinity-purified using streptavidin-agarose beads. Zones within the red rectangles were excised, proteins were digested with trypsin and analyzed using LC-MS/MS.

Figure 9 Mass Spectrometric Detection of HvPap-6

HvPap-6

Top fraction

MEKKSTAATQSIPTATPLFLGDAPLVSGMRTSMALLAASAALLMVSLAAAADMSIVSYGERSEEEVRR
 MYAEWMAEHGSTYNAIGEEERRFEAFRDNLRYIDQHNAADAGVHSFRLGLNRFADLTNEEYRSTYLGR
 TKPDRERKLSARYQAADNDLPESEVDWRKKGAVGAVKDQGGCGSCWAFSAIAAVEGINQIVTGDMLPSE
 QELVDCDTSYNGCGNGGLMDYAFEFIINNNGGIDSEEDYPYKERDNRCDANKKNKVVTTIDGYEDVPVNSE
 KSLQKAVANQPIISVAIEAGGRAFQLYKSGIFTGTCGTALDHGVAAVGYGTENGKDYWLVRNSWGSVWGED
 GYIRMERNIKASSGKCGIAVEPSYPTKTGENPPNPGTPPSPAPPSSVCDSENECPASTTCCCIYEYGE
 CFAWGCCPLEGATCCDDHYSPPHNYICNTKQGTCLAAKDSPLSVKAQRRTLAKPIGAFSGIAIDGKKS
 SA

Middle fraction

MEKKSTAATQSIPTATPLFLGDAPLVSGMRTSMALLAASAALLMVSLAAAADMSIVSYGERSEEEVRR
 MYAEWMAEHGSTYNAIGEEERRFEAFRDNLRYIDQHNAADAGVHSFRLGLNRFADLTNEEYRSTYLGR
 TKPDRERKLSARYQAADNDLPESEVDWRKKGAVGAVKDQGGCGSCWAFSAIAAVEGINQIVTGDMLPSE
 QELVDCDTSYNGCGNGGLMDYAFEFIINNNGGIDSEEDYPYKERDNRCDANKKNKVVTTIDGYEDVPVNSE
 KSLQKAVANQPIISVAIEAGGRAFQLYKSGIFTGTCGTALDHGVAAVGYGTENGKDYWLVRNSWGSVWGED
 GYIRMERNIKASSGKCGIAVEPSYPTKTGENPPNPGTPPSPAPPSSVCDSENECPASTTCCCIYEYGE
 CFAWGCCPLEGATCCDDHYSPPHNYICNTKQGTCLAAKDSPLSVKAQRRTLAKPIGAFSGIAIDGKKS
 SA

Bottom fraction

MEKKSTAATQSIPTATPLFLGDAPLVSGMRTSMALLAASAALLMVSLAAAADMSIVSYGERSEEEVRR
 MYAEWMAEHGSTYNAIGEEERRFEAFRDNLRYIDQHNAADAGVHSFRLGLNRFADLTNEEYRSTYLGR
 TKPDRERKLSARYQAADNDLPESEVDWRKKGAVGAVKDQGGCGSCWAFSAIAAVEGINQIVTGDMLPSE
 QELVDCDTSYNGCGNGGLMDYAFEFIINNNGGIDSEEDYPYKERDNRCDANKKNKVVTTIDGYEDVPVNSE
 KSLQKAVANQPIISVAIEAGGRAFQLYKSGIFTGTCGTALDHGVAAVGYGTENGKDYWLVRNSWGSVWGED
 GYIRMERNIKASSGKCGIAVEPSYPTKTGENPPNPGTPPSPAPPSSVCDSENECPASTTCCCIYEYGE
 CFAWGCCPLEGATCCDDHYSPPHNYICNTKQGTCLAAKDSPLSVKAQRRTLAKPIGAFSGIAIDGKKS
 SA

Once Twice Three times Four times Five times Six times

Figure 9. Mass spectrometric detection of HvPap-6. The three gel fractions delineated in Fig. 14 were digested with trypsin and analyzed by LC-MS/MS. Colors indicate how often a particular protein region was detected in different (overlapping) peptides.

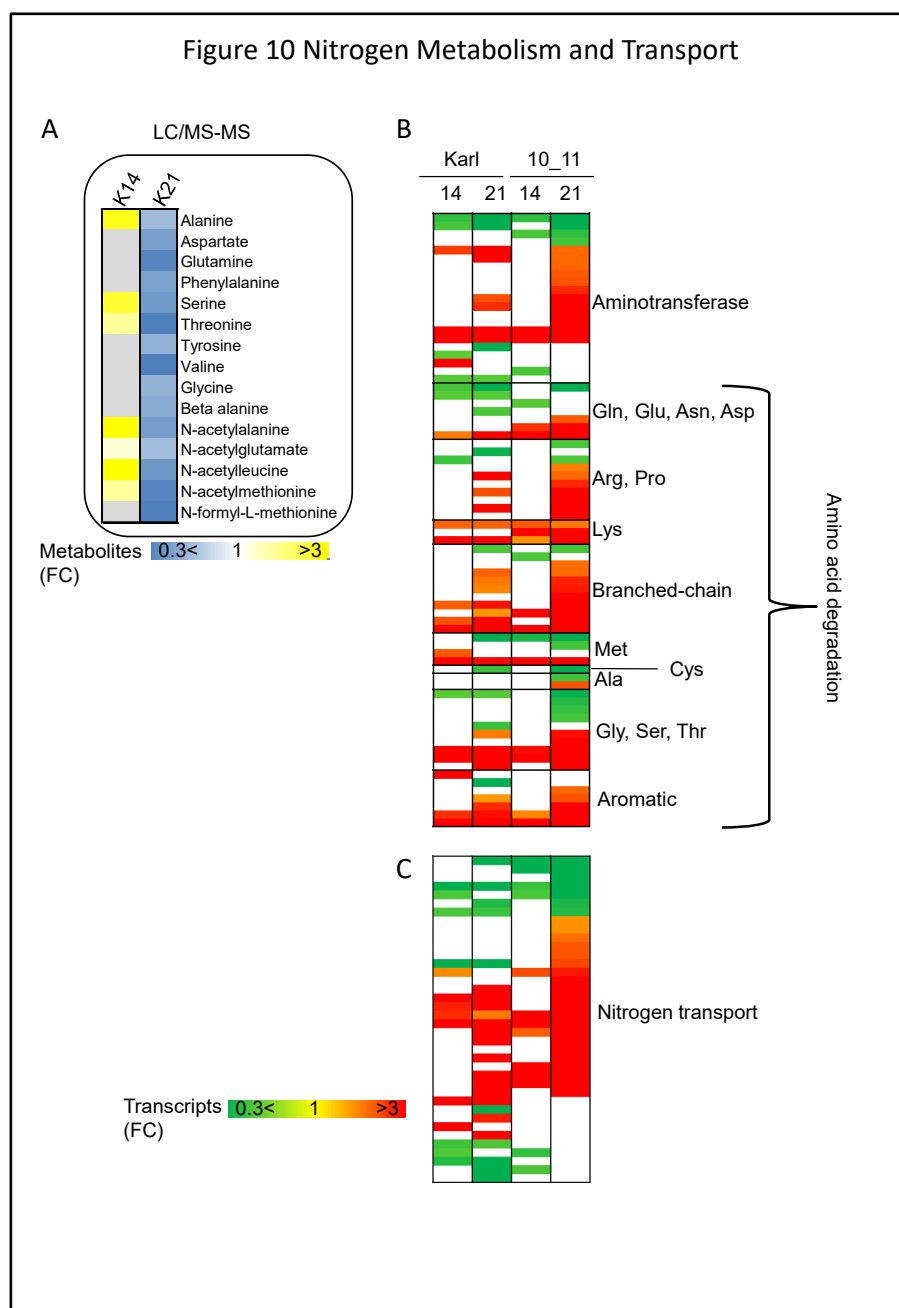


Figure 10. Nitrogen metabolism and transport. Marseq analysis was performed on senescing flag leaves from cv. 'Karl' and its near-isogenic line '10-11' at 7, 14 and 21 days past anthesis (dpa). The expression profiles of genes coding for enzymes and proteins involved in transamination, amino acid degradation and nitrogen transport were inspected (panels B and C). Values represent –fold changes (FC) at 14 vs. 7 dpa, and at 21 vs 7 dpa. Values >1 indicate upregulation at the later time point, i.e., with progressing leaf senescence. Only genes/time points with FC >1.8 or FC <0.55 with $p < 0.05$ are shown. Metabolite (amino acid) profiling (panel A) was performed on senescing flag leaves from cv. 'Karl' at 7, 14 and 21 dpa; data are presented as for transcripts.

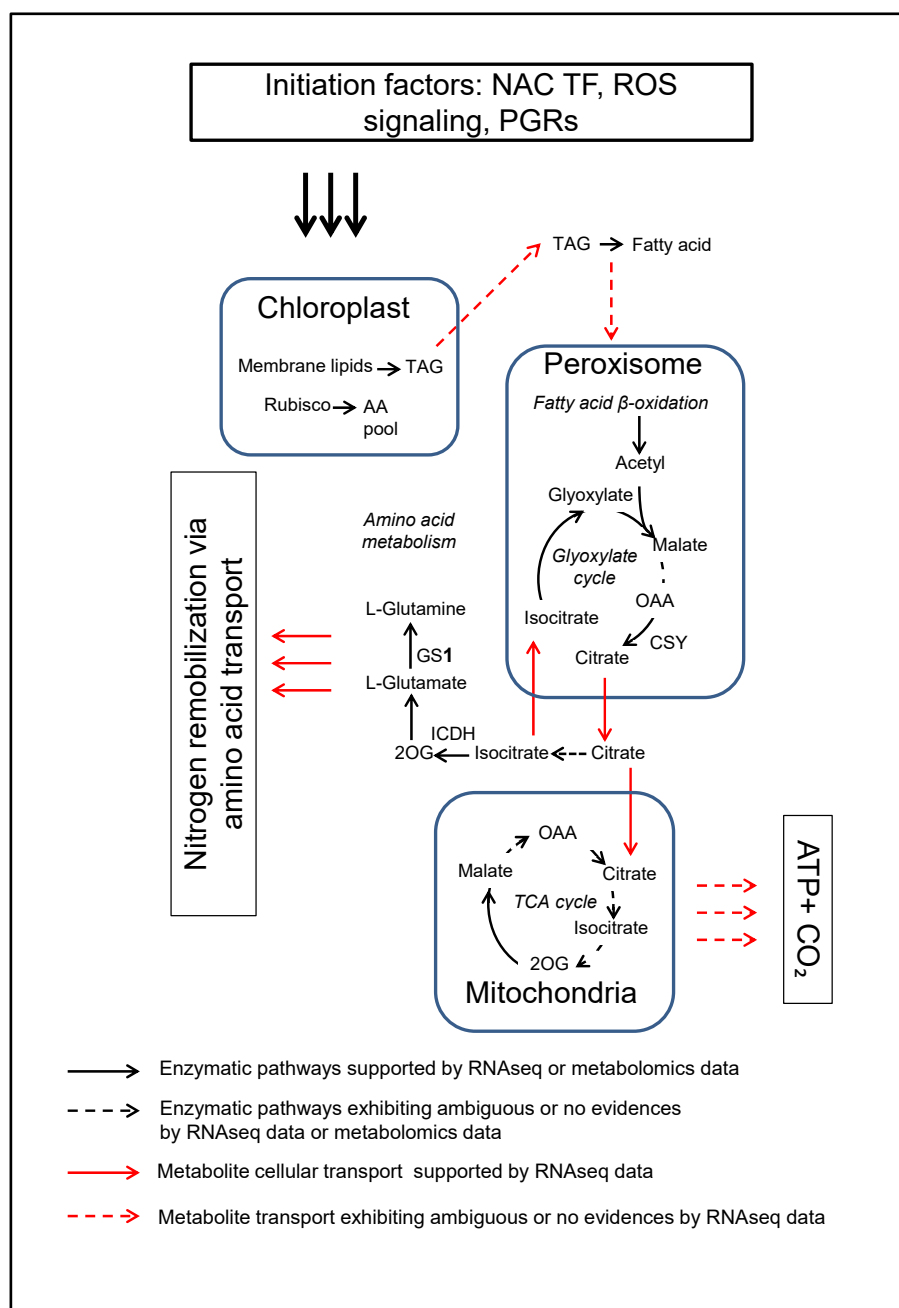


Figure 11: Proposed model of energy control and nitrogen remobilization during senescence. Initiation factors such as NAC transcription factors, ROS signaling compounds and hormones (perhaps JA or signaling molecules related to JA) orchestrate the downregulation of photosynthesis and dismantling of the chloroplast. As a result, proteolytic activity increases releasing amino acids, and membrane lipids are converted to triacylglycerols (TAGs). TAGs are converted to fatty acids and used as substrates by the β-oxidation pathway for the production of acetyl-CoA necessary for the TCA and glyoxylate cycles. Citrate generated as part of the glyoxylate cycle can be transported to the cytosol or to the mitochondria to be converted to 2-oxoglutarate (2OG). This metabolite is further needed in amino acid metabolism, producing glutamate and glutamine. Glutamine is transported to sink organs, involving leaf amino acid transporters.